Dalton Transactions

RSC Publishing

PAPER

View Article Online
View Journal | View Issue

Cite this: *Dalton Trans.*, 2013, **42**, 4291

Reversible binding of water, methanol, and ethanol to a five-coordinate ruthenium(II) complex†

Erin S. F. Ma, Brian O. Patrick and Brian R. James*

Received 4th December 2012,
Accepted 8th January 2013

DOI: 10.1039/c3dt32909g

www.rsc.org/dalton

The known green, five-coordinate, square-pyramidal *trans*-$RuCl_2$(P–N)(PPh_3) complex reversibly binds water, MeOH and EtOH in the vacant coordination site in the solid state and in CH_2Cl_2 solution to give pink adducts (P–N = *o*-diphenylphosphino-*N*,*N*′-dimethylaniline). The adducts are well characterized, including X-ray analysis of the aqua complex, *trans*-$RuCl_2$(P–N)(PPh_3)(H_2O), which crystallizes in two different benzene-solvated forms. Comparison of the structural data with those determined previously for the binding of H_2S, thiols, and H_2, which form *cis*-RuX_2(P–N)(PPh_3)L products (X = Cl, Br; L = a S-ligand or H_2) reveals the *trans*-influence trend P > H_2S ~ thiols > H_2 > Cl ~ Br > H_2O. Thermodynamic data for the binding of water were estimated in solution by UV-Vis spectroscopy, and ΔH^o data for the aqua and alcohol adducts in the solid state were obtained by differential scanning calorimetry. Inclusion of published data for the S-ligand adducts reveals the thermal stability trend of the solid complexes as MeSH > MeOH > H_2S > H_2O > EtSH > EtOH.

Introduction

We recently published details on the reversible binding in solution of H_2S and alkyl thiols to five-coordinate complexes of the type *trans*-RuX_2(P–N)(PR_3) where P–N = *o*-diphenylphosphino-*N*,*N*′-dimethylaniline, X = halide, and R = Ph or *p*-tolyl (*cf.* eqn (1)); thermodynamic data were also presented for formation of some selected H_2S, MeSH and EtSH products, in which the halide ligands are now *cis*.[1] In publications from the 1990s,[2] we had mentioned corresponding coordination of MeOH, EtOH and H_2O but the details have been available only in Ph.D. dissertations.[3] This current paper now describes the alcohol and aqua products, which have *trans*-chlorides (eqn (1)). The findings include crystallographic data for the aqua complexes, and thermodynamic data for reversible binding of these O-donors, which allow for comparison with data for the S-donor ligand systems.

Department of Chemistry, University of British Columbia, Vancouver, British Columbia, Canada, V6T 1Z1. E-mail: brj@chem.ubc.ca

†Electronic supplementary information (ESI) available: ORTEP of **2b**; TGA of **2a**; $^{31}P\{^1H\}$- and ^1H-NMR spectra of **2a** at different temperatures; $^{31}P\{^1H\}$ and UV-vis spectral changes on addition of H_2O to **1a** to form **2a**, and data for determination of thermodynamic data for this reaction; ^1H NMR spectrum of **3**. CCDC 913686 and 913687. For ESI and crystallographic data in CIF or other electronic format see DOI: 10.1039/c3dt32909g

Experimental section

General

Unless stated otherwise, all manipulations were performed under an oxygen-free Ar or N_2 atmosphere at ambient temperatures using standard Schlenk techniques. Commercially available compounds were supplied by Aldrich or Fisher, and were used as received unless stated otherwise. Spectral or analytical grade solvents were refluxed, distilled over appropriate drying agents,[4] and then purged with Ar or N_2 before being transferred into a reaction flask *via* a cannula. Deuterated solvents, obtained from Cambridge Isotope Laboratories, were stored over activated molecular sieves (Fisher 4 Å, 4–8 mesh), and immediately before use were de-oxygenated (*via* the freeze–pump–thaw method), and stored under Ar.

NMR spectra were recorded, unless stated otherwise, at room temperature (r.t. ~22 °C) on Varian XL300 (300.0 MHz for ^1H, 121.4 MHz for ^{31}P) or Bruker AMX500 (500.0 MHz for ^1H and 202.5 MHz for ^{31}P) instruments. Residual deuterated solvent protons (relative to external $SiMe_4$) and external $P(OMe)_3$ (δ 141.0 relative to 85% H_3PO_4) were used as references (s = singlet, d = doublet, t = triplet, q = quartet, m = multiplet, br = broad); *J* values are reported in hertz (Hz). Samples were prepared in 5 mm NMR tubes equipped with poly(tetrafluoroethylene), J.-Young valves (Aldrich). Calibrated ^1H NMR probes were used to determine the temperatures used for van't Hoff analysis. ATLI Mattson Genesis FTIR and Bomem Michelson far-IR spectrophotometers were used to record spectra from 500–4000 cm^{-1} (KBr) and 200–3000 cm^{-1} (CsI); data are

reported in cm^{-1}. UV-Vis spectra were recorded on a Hewlett Packard 8452A diode-array spectrophotometer, equipped with a thermostated compartment using an anaerobic, 1 cm quartz cell, joined to a side-arm flask for mixing solutions; data are reported as λ_{max} in nm (ε in units of M^{-1} cm^{-1}). Thermogravimetric analysis (TGA) was performed on a TA Q50 Instrument: solid samples were weighed (10 to 15 mg) into a Pt pan, and the samples were then heated under N_2 (flow rate = 100 cc min^{-1}) at a rate of 10 °C min^{-1} to ~500 °C. Differential scanning calorimetry (DSC) data were collected on a TA 910S Instrument, with 2–5 mg samples being heated under N_2 (flow rate = 40 cc min^{-1}) at a rate of 5 °C min^{-1} up to 500 °C. Microanalyses were performed in this department on a Carlo Erba 1106 instrument.

The $RuCl_2(PR_3)_3$ (R = Ph,[5] *p*-tolyl[6]), $RuCl_2$(P–N)(PPh_3) (**1a**),[2a] and $RuCl_2$(P–N)(P(*p*-tolyl)$_3$) (**1b**)[2a] complexes were prepared by the literature methods, the precursor $RuCl_3{\cdot}xH_2O$ being donated by Colonial Metals, Inc.

***trans*-$RuCl_2$(P–N)(PPh_3)(H_2O) (2a).** The complex was prepared by adding a mixture of H_2O (2 mL) and acetone (2 mL) to a stirred solution of $RuCl_2(PPh_3)_3$ (200 mg, 0.21 mmol) and P–N (64 mg, 0.21 mmol) in acetone (5 mL) at r.t. The instantly formed orange-pink solution was stirred for 3 h during which time a pink solid precipitated; this was filtered off, washed with acetone (2 × 5 mL), and dried *in vacuo* for 24 h. Yield: 115 mg, 73%. Anal. Calcd $C_{38}H_{37}NOCl_2P_2Ru{\cdot}$(acetone): C, 60.37; H, 5.31; N, 1.72. Found: C, 60.37; H, 5.46; N, 1.67. $^{31}P\{^1H\}$ NMR (C_6D_6): δ 73.52 (d, *P*–N), 49.30 (d, *P*Ph_3); $^2J_{PP}$ = 38.0. ^1H NMR (C_6D_6): δ 8.4–7.0 (29H, m, Ph), 3.05 (6H, s, N(CH_3)$_2$), 2.15 (2H, br s, Ru–OH_2), 1.55 (6H, s, acetone). UV-Vis (see Results and discussion). IR: ν_{OH} 3556 s, 3295 s, 1605 s, ν_{CO} 1707 s (acetone). Two different type crystals (**2a**·2C_6H_6 and **2a**·1.5C_6H_6) were isolated from evaporation of a saturated C_6H_6 solution of the complex over 24 h (see X-Ray crystallographic analyses). Complex **2a** was also readily prepared *in situ* by adding one mole equiv. of H_2O (0.70 μL, 0.04 mmol) to a green $CDCl_3$ solution (0.8 mL) of precursor **1a** (29.6 mg, 0.04 mmol); the NMR data were essentially the same as those of isolated **2a**.

***trans*-$RuCl_2$(P–N)(P(*p*-tolyl)$_3$)(H_2O) (2b).** The complex was prepared in the same manner as described for **2a**, but using $RuCl_2$(P(*p*-tolyl)$_3$)$_3$ (200 mg, 0.19 mmol) as precursor. Yield: 122 mg, 77%. Anal. Calcd $C_{41}H_{43}NCl_2OP_2Ru{\cdot}$(acetone): C, 61.61; H, 5.76; N, 1.63. Found: C, 62.0; H, 5.7; N, 1.8. $^{31}P\{^1H\}$ NMR (C_6D_6): δ 63.63 (d, *P*–N), 45.91 (d, *P*Ph_3); $^2J_{PP}$ = 38.1. ^1H NMR (C_6D_6): δ 8.2–6.8 (26H, m, Ph), 3.10 (6H, s, N(CH_3)$_2$), 2.00 (3H, s, *p*-CH_3), 2.15 (2H, br s, Ru–OH_2), 1.55 (6H, s, acetone). Complex **2b** can also be made *in situ* by a 1 : 1 reaction of H_2O with **1b** in $CDCl_3$, as noted above for **2a**.

***trans*-$RuCl_2$(P–N)(PPh_3)(MeOH) (3).** A mixture of MeOH (2 mL) and acetone (1 mL) was purged with Ar and cannula transferred to a stirred solution of $RuCl_2(PPh_3)_3$ (100 mg, 0.10 mmol) and P–N (32 mg, 0.10 mmol) in acetone (5 mL), which had been heated to 50 °C. The instantly formed orange solution was stirred at 20 °C for 24 h, and the volume was then reduced to ~1 mL, when hexanes (10 mL) was added to precipitate a pink solid; this was collected, washed with MeOH (2 × 5 mL), and dried by passing Ar through the sample at r.t. for ~15 min. Yield: 45 mg, 56%. Anal. Calcd $C_{39}H_{39}NOCl_2P_2Ru$: C, 60.70; H, 5.09; N, 1.82. Found: C, 61.0; H, 5.1; N, 1.8. $^{31}P\{^1H\}$ NMR (CD_2Cl_2): δ 77.46 (d, *P*–N), 47.16 (d, *P*Ph_3); $^2J_{PP}$ = 36.7. ^1H NMR (CD_2Cl_2): δ 7.9–6.9 (29H, m, Ph), 3.33 (3H, d, OCH_3), 3.16 (6H, s, N(CH_3)$_2$), 1.33 (1H, q, O*H*).

***trans*-$RuCl_2$(P–N)(PPh_3)(EtOH) (4).** Attempts to prepare **4** by the method described for **3** were unsuccessful. Several different solvent combinations, including acetone mixtures with Et_2O, EtOH or hexanes, failed to precipitate any solid. When P–N (40.5 mg, 0.13 mmol) in EtOH (2 mL) was added to a brown suspension of $RuCl_2(PPh_3)_3$ (122.8 mg, 0.13 mmol) in EtOH (8 mL), and the mixture stirred for 1 week, an orange-pink solution containing a small amount of a light brown precipitate formed. This solid (~20 mg) was collected and washed with EtOH (5 mL), but it was insoluble in common solvents (acetone, $CDCl_3$, C_6D_6, CD_2Cl_2). Also, the EtOH was removed under vacuum from the pink filtrates, and hexanes (10 mL) was then added to the oily residue. The solvent was again removed and EtOH (2 mL) was added to dissolve the residue; stirring for 15 min generated a pink precipitate. Hexanes (10 mL) was then added to precipitate more solid, which was collected by filtration, washed with hexanes (5 mL), and drying attempted by using an Ar stream as for **3**. Yield: 33 mg, 33%. Anal. Calcd $C_{40}H_{41}NOCl_2P_2Ru$: C, 61.15; H, 5.26; N, 1.78. Found: C, 62.2; H, 5.1; N, 1.9. $^{31}P\{^1H\}$ NMR (CD_2Cl_2): δ 79.79 (d, *P*–N), 46.90 (d, *P*Ph_3); $^2J_{PP}$ = 36.2. ^1H NMR (CD_2Cl_2): δ 7.9–6.9 (29H, m, Ph), 3.61 (2H, d of q, OCH_2), 3.18 (6H, s, N(CH_3)$_2$), 1.40 (1H, t, O*H*)), 1.16 (3H, t, OCH$_2$CH_3).

X-Ray crystallographic analyses

X-ray analyses of **2a**·2C_6H_6 and **2a**·1.5C_6H_6 were carried out at 180 K on a Rigaku/ADSC CCD area detector with graphite monochromated MoKα radiation (0.71069 Å). The crystals differ in appearance as well as having different unit cells, the pink crystals (**2a**·2C_6H_6) being monoclinic, and the yellow-brown crystals (**2a**·1.5C_6H_6) being triclinic. Some crystallographic data for the **2a**·2C_6H_6 structure are: 38 827 total reflections, 10 710 unique (R_{int} = 0.074), 6767 observed [$I > 2\sigma(I)$], R_1 = 0.076; wR_2 = 0.167; GOF = 1.11; residual density = −1.39 e $Å^{-3}$. Corresponding data for **2a**·1.5C_6H_6 are: 18577, 9156 (0.039), 6959, 0.062, 0.098, 1.01, and −0.0.87. Data were processed using the d*TREK area detector program,[7] and the structures were solved by direct methods.[8] All refinements were performed using the SHELXL-97 program[9] *via* the WinGX interface.[10] For both structures, all non H-atoms were refined anisotropically; the H-atoms of the coordinated H_2O were located in a difference map and refined isotropically. All other H-atoms were placed in calculated positions. For the crystals with the 1.5 molecules of C_6H_6 in the asymmetric unit, one half-benzene resides on an inversion centre, while within the material with two C_6H_6 molecules, one was disordered and was modeled in three orientations such that their combined occupancies summed to 1.0. The ORTEP plots and selected bond lengths and angles of the **2a** structures are shown in Fig. 1 and 2, and Tables 1 and 2, while the full experimental

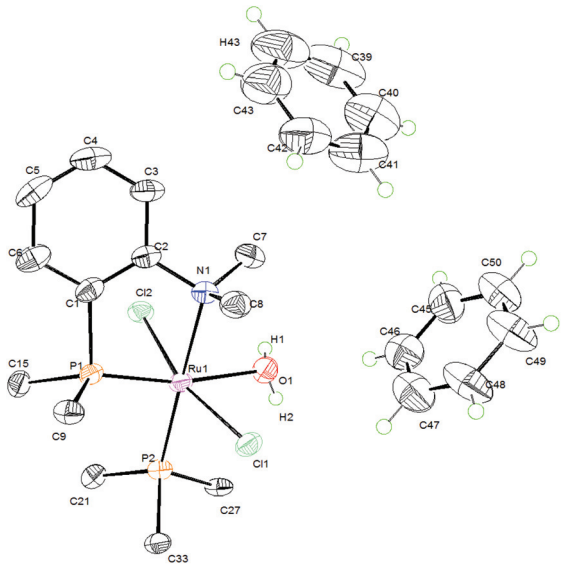

Fig. 1 ORTEP diagram of *trans*-$RuCl_2$(P–N)(PPh_3)(H_2O) (**2a**·$2C_6H_6$) with 50% probability thermal ellipsoids.

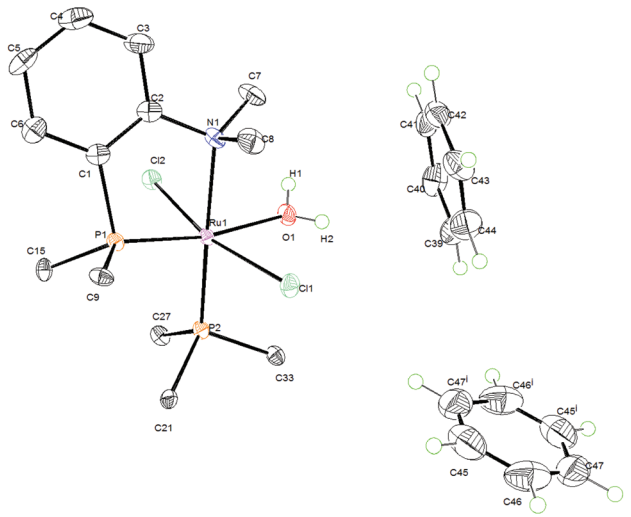

Fig. 2 ORTEP diagram of *trans*-$RuCl_2$(P–N)(PPh_3)(H_2O) (**2a**·$1.5C_6H_6$) with 50% probability thermal ellipsoids.

Table 1 Selected bond lengths (Å) for benzene solvated *trans*-$RuCl_2$(P–N)(PPh_3)(H_2O) (**2a**·$2C_6H_6$ and **2a**·$1.5C_6H_6$), and *trans*-$RuCl_2$(P–N)(P(*p*-tolyl)$_3$)(H_2O) (**2b**), with estimated standard deviations in parentheses

Bond	**2a**·$2C_6H_6$	**2a**·$1.5C_6H_6$	**2b**
Ru(1)–O(1)	2.232(4)	2.191(2)	2.252(4)
Ru(1)–P(1)	2.2305(14)	2.2333(8)	2.220(1)
Ru(1)–P(2)	2.3143(14)	2.3091(7)	2.284(1)
Ru(1)–N(1)	2.312(4)	2.311(2)	2.326(4)
Ru(1)–Cl(1)	2.3957(13)	2.4311(7)	2.385(1)
Ru(1)–Cl(2)	2.4195(13)	2.3951(7)	2.418(1)
O(1)–H(1)	0.870(10)	0.863(10)	0.69(6)
O(1)–H(2)	0.870(10)	0.866(10)	0.96(6)
H(1)···Cl(2)	2.27(7)	2.31(3)	2.46(7)

Table 2 Selected bond angles (°) for benzene solvated *trans*-$RuCl_2$(P–N)(PPh_3)(H_2O) (**2a**·$2C_6H_6$ and **2a**·$1.5C_6H_6$), and *trans*-$RuCl_2$(P–N)(P(*p*-tolyl)$_3$)(H_2O) (**2b**), with estimated standard deviations in parentheses

Bond	**2a**·$2C_6H_6$	**2a**·$1.5C_6H_6$	**2b**
H(1)–O(1)–H(2)	107(3)	109(3)	111(6)
Ru(1)–O(1)–H(1)	118(6)	121(3)	112(4)
Ru(1)–O(1)–H(2)	114(6)	115(3)	105(6)
Cl(1)–Ru(1)–O(1)	82.62(11)	80.76(6)	81.6(1)
Cl(2)–Ru(1)–O(1)	83.67(11)	85.26(6)	82.2(1)
Cl(1)–Ru(1)–P(1)	104.20(5)	105.31(3)	104.30(5)
Cl(1)–Ru(1)–P(2)	86.94(5)	86.98(2)	89.74(5)
Cl(1)–Ru(1)–N(1)	91.09(11)	92.27(6)	90.8(1)
Cl(1)–Ru(1)–Cl(2)	165.17(5)	165.58(2)	162.91(4)
O(1)–Ru(1)–P(1)	168.22(11)	169.78(6)	168.8(1)
O(1)–Ru(1)–P(2)	90.87(11)	88.69(6)	91.4(1)
O(1)–Ru(1)–N(1)	88.90(16)	90.32(8)	90.3(1)
Cl(2)–Ru(1)–P(1)	88.43(5)	88.04(3)	90.73(4)
Cl(2)–Ru(1)–P(2)	98.89(5)	96.26(2)	96.26(5)
Cl(2)–Ru(1)–N(1)	83.03(11)	84.25(6)	83.7(1)
P(1)–Ru(1)–P(2)	98.99(5)	99.71(3)	98.04(5)
P(1)–Ru(1)–N(1)	81.46(11)	81.33(6)	80.20(9)
P(2)–Ru(1)–N(1)	178.03(12)	178.85(6)	178.24(9)

parameters and details of the two structures are given in CIF format in the ESI.†

Reddish crystals of **2b**, deposited over 3 h in the NMR tube of an *in situ* synthesis, were analysed crystallographically at r.t. in 1994 as a non-solvated molecule on a Rigaku AFC6S instrument with CuKα radiation. An ORTEP structure (Fig. S1†) and crystallographic details (Appendix A, in non-CIF format) are given in the ESI;† some bond lengths and angles are also given in Tables 1 and 2.

Results and discussion

The aquo complexes

The coordination chemistry of H_2O is ubiquitous, although after an extensive search we have been unable to find any report on formation of a neutral, six-coordinate Ru^{II}-aqua complex *via* reaction of H_2O with a five-coordinate precursor, as exemplified here in eqn (1) by the reactivity of the $RuCl_2$(P–N)(PR_3) complexes (R = Ph, **1a**; *p*-tolyl, **1b**); the aqua product, like the precursor, has *trans*-chlorides. As mentioned in the Introduction, H_2S (and thiols) similarly coordinate, but the isolated product with these S-ligands has *cis*-chlorides with the H_2S *trans* to a Cl.[1] Of note, however, there is a recent example of reversible addition of H_2O to a cationic, five-coordinate RuCl(PNNP)$^+$ complex to give a mixture of *cis*- and *trans*-products, where the P-atoms (and the N-atoms) occupy *cis*-positions within the tetradentate ligand.[11]

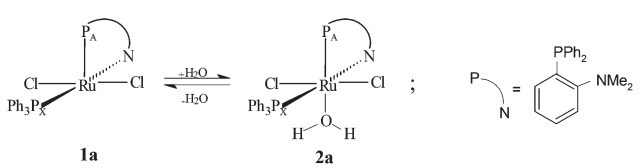

(1)

The air-sensitive, pink complexes (**2a** and **2b**) can be prepared by stirring **1a** and **1b** in a 4 : 1 mixture of acetone and

H_2O under Ar at r.t., the products being isolated as the solvated *trans*-$RuCl_2$(P–N)$(PR_3)(H_2O)$·(acetone) complexes (R = Ph, *p*-tolyl). More conveniently, the required unsaturated, green precursor species (**1a**/**1b**) can be formed *in situ* from P–N and $RuCl_2(PR_3)_3$, as described in the Experimental section. Heating **2a**/**2b** *in vacuo* at 80 °C regenerates **1a**/**1b**. The loss of H_2O was confirmed by the TGA of **2a** (Fig. S2†), where a weight loss of 11% between 80 to 110 °C, prior to thermal decomposition, agrees well with the theoretical combined 9% weight of acetone and H_2O present. Exposure of **1a** and **1b** to a moist, oxygen-free atmosphere reversibly gives within minutes the aqua species, with formation of **2b** (<3 min) being noticeably faster (*via* colour change) than **2a** (>15 min). The faster rate with **1b** may be related to particle size, but the X-ray structure of **1b** shows no agostic interaction between the Ru and an *o*-phenyl H-atom from the P(*p*-tolyl)$_3$ ligand,[2a] and thus the species does have an easily accessible, vacant coordination site; the implication is that **1a** might show such an interaction, but unfortunately many attempts to grow crystals of this complex were unsuccessful.

The structures of **2a** in both solvate forms and **2b** (Fig. 1, 2 and S1;† Tables 1 and 2) reveal pseudo-octahedral geometry at the Ru with *trans*-chlorides, with the H_2O being *trans* to the P-atom of the P–N ligand; the H-atoms of the H_2O were isotropically refined in the structures. The non-disordered crystals of **2a**·1.5C_6H_6 revealed a 2.77(3) Å distance between the aqua H(2) and benzene C(40), suggesting an OH/π-benzene ring interaction. This possibly results in the observed shorter Ru–O bond in **2a**·1.5C_6H_6 than in **2a**·2C_6H_6 by ~0.04 Å. The value is intermediate between those of a relatively weakly bound aqua ligand [*e.g.*, 2.215 Å in *cis*-$[RuCl(H_2O)(PNNP)]^+$ mentioned above,[11] 2.218 Å in *trans*-$[Ru(H_2O)(PEt_3)_2(trpy)]^{2+}$ (trpy = 2,2′,2″-terpyridine)[12a] and 2.203 Å in $[Ru(\eta^6\text{-}p\text{-}MeC_6H_4{}^iPr)(H_2O)L]^+$ (HL = *S*-(α-methylbenzyl)-salicylaldimine)[12b]] and a more strongly bound one [*e.g.* 2.15 Å in $[RuH(H_2O)(CO)_2(PPh_3)_2]^+$,[13] 2.127 Å in $[Ru(\eta^6\text{-}C_6H_6)(H_2O)_3]^{2+}$,[14] 2.141 and 2.115 Å in $Ru(H_2O)_2(\eta^1(O){:}\eta^2(C,C')\text{–}OCOCH_2CH{=}CHCH_3)_2$,[15] 2.122 Å in $[Ru(H_2O)_6]^{2+}$,[16] and 2.158 and 2.095 Å in $[Ru(cod)(H_2O)_4]^{2+}$ [17]]; there are several other examples within cationic Ru^{II} systems.[11] The shorter Ru–O bonds in **2a**·1.5C_6H_6 and **2a**·2C_6H_6 relative to the one in **2b** perhaps contributes to a greater interaction between H(1)···Cl(2) in the **2a** species. Of note, the O–H bonds are up to ~0.25 Å shorter than the 0.956 Å value in free H_2O, while the approximate H–O–H angles are somewhat greater than that of free H_2O (105°); the weak OH···benzene and OH···Cl interactions almost certainly play a role. In the H_2S analogue of **2a**, isolated as an acetone solvate in which H-bonding to a chloride is also present,[20] the H–S–H angle 102(2)° is larger than that of free H_2S (92.5°), and the Ru–S bond length (2.35 Å) is as expected longer than the Ru–O bond in the aqua species. The non-linear Cl–Ru–Cl angles (~165 Å) in the **2a** and **2b** structures must result from the bending of the chlorides towards the aqua ligand due to H-bonding interactions, which are thought more generally (even in non-chloro-containing species) to stabilize Ru^{II}-aqua complexes.[11]

As noted above, the *trans*-$RuCl_2$(P–N)(PR_3) precursors bind H_2S, MeSH and EtSH to form *cis*-$RuCl_2$(P–N)(PR_3)L products (L = the S-donor),[1] and the P(1) of the P–N ligand, like L, is also *trans* to a Cl-atom. In the aqua species, P(1) is *trans* to H_2O, and the Ru–P(1) bonds in **2a**·2C_6H_6, **2a**·1.5C_6H_6 and **2b** (2.231, 2.233, and 2.220 Å, respectively) are shorter than the average value of 2.27 Å for the S-containing complexes, indicating that Cl has a stronger *trans*-influence than H_2O toward a phosphine P-atom; this agrees with *ab initio* calculations,[18] and $^1J_{PtP}$ NMR data for *trans*-$[Pt(H_2O)(CH_3)(diphos)]^+$ and *trans*-$[PtCl(CH_3)(diphos)]$.[19] The correlation between ^{31}P NMR data and *trans*-influence will be further discussed below.

The NMR data in C_6D_6 for the aqua-adducts: an AX $^{31}P\{^1H\}$ pattern with δP_A of the P–N ligand (eqn (1)) being at lower field (by ~17–25 ppm) than δP_X with ^2J ~ 38 Hz, and singlets at δ_H ~ 3.50–3.00 in the ^1H spectrum for equivalent NMe_2 groups,[1] are consistent with the solid state structures. The resolution and shifts of the NMR resonances for the aqua-adducts are, however, dependent on the solvent, temperature and concentration of added H_2O. Because of the rapid equilibrium (eqn (1)), some of the resonances of **2a** and **1a** are broadened on the NMR-timescale. The sharp doublets at δP_X ~ 48 for **2a** are little affected but, for example on dissolution of **2a** in CD_2Cl_2 (Fig. S3†), the composite broadened P_A signal changes from ~80 to 62 ppm on going from 25 to −80 °C: at 25 °C, **1a** is favoured (δP_A 80.1). At −50 °C, the concentrations of **1a** and **2a** must be similar as the resonances coalesce into the base line, and at −80 °C, **2a** dominates. Such coalescence resulting from the *trans*-effect of a P-atom on a H_2O ligand has been noted previously within the weakly bonded aqua complexes, *trans*, *mer*-$[MCl_2(H_2O)(PMe_2Ph)_3][ClO_4]$ (M = Rh[21] or Ir[22]). Table S1† gives the $^{31}P\{^1H\}$ data for **1a** and isolated samples of **2a** at r.t. in various solvents. Fig. S4† clearly shows that increasing [H_2O] is required to fully form **2a** in d_6-acetone where, in the absence of H_2O, **1a** exists as the acetone adduct:[1] with increasing [H_2O], the broadened doublet P_A signal at δ 70.5 gradually becomes the sharp doublet of **2a** at ≥300 equiv. of H_2O, while the sharp P_X doublet changes little. The ^1H NMR spectra of **2a** in various solvents are consistent with the $^{31}P\{^1H\}$ data, although the distinction between the resonances of **2a** and **1a** is not as obvious. For example, in CD_2Cl_2 solutions of **2a**, the NMe_2 signals of **2a** and **1a** overlap as seen in Fig. S5;† of note, when the solution is cooled from 25 to −80 °C, the Ru–OH_2 signal moves downfield from δ 2.18 to 3.42, whereas the NMe_2 signals shift upfield from δ 3.20 to 2.85. In *cis*-$RuCl_2$(P– N)(PR_3)L complexes, where L is H_2S, MeSH, EtSH or H_2 [1,2a,3b] the two Me groups are inequivalent as established by crystallographic and ^1H data.

The $^{31}P\{^1H\}$ and ^1H NMR spectra for the **1a**/**2a** equilibrium contrast with those of the corresponding reversible binding of S-ligands to give *cis*-products, where under similar conditions both **1a** and the H_2S- and RSH-adducts, for example, are readily distinguished by ^1H NMR data, and equilibria and thermodynamic data for the reversible binding could be obtained by these data.[1] The aqua system is clearly much more labile on the NMR-timescale compared to the H_2S system; however,

Table 3 Comparison of $^{31}P\{^{1}H\}$ NMR data and Ru–P bond lengths (in Å)

Complex (in $CDCl_3$ at 20 °C)[a]	δP_A	Ru–P_A	δP_X	Ru–P_X	$^2J_{PP}$ (Hz)
t-$RuCl_2$(P–N)(P(*p*-tolyl)$_3$) (**1b**)[b]	81.46	2.170(1)	47.64	2.290(1)	37.15
t-$RuCl_2$(P–N)(P(*p*-tolyl)$_3$)(H_2O) (**2b**)[c]	71.80	2.220(1)	47.62	2.284(1)	38.12
t-$RuCl_2$(P–N)(PPh_3)(H_2O) (**2a**·2C_6H_6)	68.50	2.2305(14)	47.70	2.3143(14)	37.76
(**2a**·1.5C_6H_6)		2.2333(8)		2.3091(7)	
c-$RuCl_2$(P–N)(P(*p*-tolyl)$_3$)(H_2S)[d] (**5**)	51.91	2.2560(4)	42.58	2.3040(3)	30.41
c-$RuCl_2$(P–N)(PPh_3)(H_2S)[e] (**6**)	50.60	2.2712(6)	44.48	2.3110(7)	30.23
c-$RuBr_2$(P–N)(PPh_3)(H_2S)[e] (**7**)	53.41	2.262(1)	44.36	2.301(1)2	29.20
c-$RuCl_2$(P–N)(PPh_3)(MeSH)[f] (**8**)	51.43	2.2802(8)	42.37	2.3109(8)	29.87
c-$RuCl_2$(P–N)(PPh_3)(EtSH)[f] (**9**)	50.97	2.2743(4)	42.48	2.3110(5)	30.05
c-$RuCl_2$(P–N)(PPh_3)(H_2)[g] (**10**)	49.30	2.2884(7)	45.48	2.3098(6)	26.83

[a] *t* = *trans*; *c* = *cis*. [b] Ref. 2*a*. [c] Ref 3*a*. [d] Ref. 2*b*. [e] Ref. 20. [f] Ref. 1. [g] Ref. 3*b*.

equilibria data for the aquo system could be determined by UV-Vis spectroscopy, a faster timescale technique (see below).

The rapid and reversible coordination of H_2O must result from the *trans*-effect of the P_A-atom on the H_2O ligand. Conversely, the *trans*-influence of the H_2O must weaken the Ru–P_A bond relative to its strength in **1a**. The *trans*-influence of the ligand *trans* to P_A is demonstrated by $^{31}P\{^{1}H\}$ NMR data for the $RuCl_2$(P–N)(PR_3)L complexes (Table 3). For example, the ligand *trans* to P_A is Cl in *cis*-$RuCl_2$(P_A–N)(P_XR_3)L, and *trans* to H_2O in *trans*-$RuCl_2$(P_A–N)(P_XR_3)(H_2O); in both species (and **1a**), the N-atom is *trans* to PPh_3 and the δP_X value of ~45 ppm is relatively insensitive to L or the orientation of the Cl-atoms (Table 3). The negligible *cis*-influence of ligands on phosphines is also well established by δ_P and $^1J_{PtP}$ values for Pt^{II}-phosphine systems.[23] The δP_A values, however, are dependent on the ligand *trans* to P_A: a more downfield P_A signal corresponds to a greater *trans*-influence of the *trans* ligand because this is determined by the ability of this ligand to deshield P_A.[24] This results from the efficacy of the ligand to compete for the metal orbital's s-character,[25] which also reflects the σ-donating ability of the ligand, as demonstrated by $^1J_{MP}$ data for M = Rh^I and Pt^{II} systems.[24b,25b,26] A larger *J* value reflects stronger σ-bonds and indicates a weaker influence of the *trans* ligand.[25b,27]

For the *cis*- and *trans*-RuX_2(P–N)(PR_3)L complexes (X = Cl, Br), the Ru–P_X bond lengths are in the 2.28–2.31 Å range (Table 3), whereas there is an inverse dependence of δP_A on the Ru–P_A length (Table 3, Fig. 3), a trend also noted for related Ru^{II}-complexes containing PPh_3[28] and $Ph_2P(CH_2)_4PPh_2$[29] ligands. Remarkably, the slopes and intercepts of all three plots (*cf.* Fig. 3) are essentially the same, about -3.0×10^{-3} Å ppm^{-1}, and ~2.43 Å, respectively. From the Fig. 3 plot, the order of decreasing *trans*-influence is Cl ~ Br > H_2O, consistent with halides being better σ- and π-donors than H_2O. Of note, $^2J_{PP}$ values for the *trans* complexes (37–38 Hz) are larger than those of the *cis* complexes (27–30 Hz). Table 4 lists the Ru–Cl bond distances for the *trans*- and *cis*-complexes: the average *trans* Ru–Cl bond distances and the Ru–Cl_A bond distances in the *cis*-species imply that S-ligands have a stronger *trans*-influence than Cl. Further, the average Ru–Cl_A value of 2.424 Å for the S-ligand *cis*-species perhaps implies a slightly greater *trans*-influence for the S-ligands than for H_2 (Ru–Cl_A = 2.409 Å). The

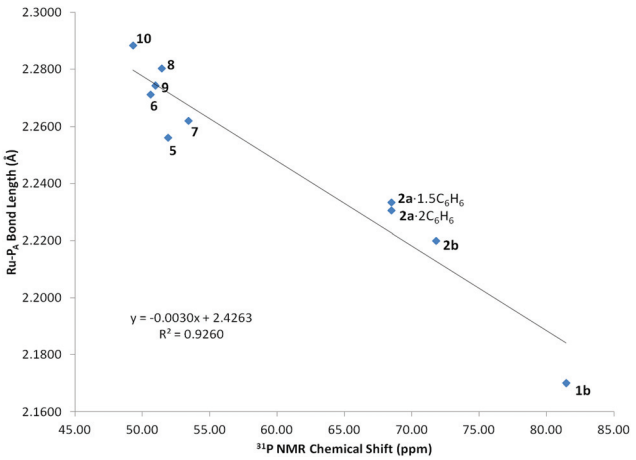

Fig. 3 Relationship between Ru–P_A bond length (Å) and δP_A (in $CDCl_3$) for the complexes listed in Table 3.

Table 4 Ru–Cl bond lengths (Å) for *cis*- and *trans*-$RuCl_2$(P–N)(PR_3)L

Complex	Ru–Cl_A	Ru–Cl_B
trans-RuCl$_2$(P–N)(PR$_3$)L		
R = *p*-tolyl, L = vacant (**1b**)	2.387(1)	2.379(1)
R = Ph, L = H_2O (**2a**·2C_6H_6)	2.3957(13)	2.4195(13)
R = Ph, L = H_2O (**2a**·1.5C_6H_6)	2.3951(7)	2.4311(7)
R = *p*-tolyl, L = H_2O (**2b**)	2.385(1)	2.418(1)
cis-RuCl$_2$(P–N)(PR$_3$)L		
R = *p*-tolyl, L = H_2S (**5**)	2.429(3)	2.469(4)
R = Ph, L = H_2S (**6**)	2.4238(6)	2.4721(5)
R = Ph, L = MeSH (**8**)	2.4241(7)	2.4472(7)
R = Ph, L = EtSH (**9**)	2.4204(6)	2.4674(5)
R = Ph, L = η^2-H_2 (**10**)	2.4090(6)	2.4543(7)

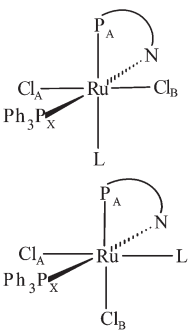

P_A-atom of the P–N ligand has a greater *trans*-influence than Cl as shown by the relatively long Ru–Cl_B bonds for the *cis*-species, consistent with the same trend already established for some Pt^{II} and Rh^I complexes.[24b,25b] Overall, assuming that *cis*-effects are negligible, the above observations suggest a *trans*-influence order of P_A > H_2S ~ thiols > H_2 > Cl ~ Br > H_2O. The trend offers plausible mechanistic insight. Formation of

trans-**2a** and -**2b** involves binding of the H_2O at the vacant position of the square pyramidal precursors (eqn (1)), whereas such coordination of the S-ligands and H_2, which give the *cis*-adducts, is likely disfavoured because of the mutual *trans*-influences of P_A and the S-ligands. Rearrangement of **2a**/**2b** to a trigonal bipyramidal intermediate with a Cl *trans* to P_A (and P_X, N and Cl in the trigonal plane), and subsequent attack at the equatorial position between P_X and N, would give the favoured *cis*-product. Such a rearrangement has been suggested previously, following dissociation of H_2O from *trans*, *mer*-$[MCl_2(H_2O)(PMe_2Ph)_3]^+$ (M = Rh[21] or Ir[30]), although routes involving initial dissociation of Cl^- are feasible.

Equilibria data for the H_2O-binding to **1a** were obtained by UV-Vis spectroscopy. The spectral changes on addition of H_2O to **1a** in CH_2Cl_2 (and in C_6H_6) to form **2a** (Fig. 4 and S6†) reveal three isosbestic points.[31] Related changes are observed when acetone and THF solutions of **1a** are used, although there are differences in the isosbestic regions (Fig. S7 and S8†) that arise because these solvents compete with H_2O for the vacant site. The equilibrium constant K for H_2O-binding in CH_2Cl_2 was estimated using eqn (2), the concentrations of **1a** and **2a** being determined from the absorbance at 678 nm (Fig. 4).

$$\log\{[\mathbf{2a}]/[\mathbf{1a}]\} = \log K + \log[H_2O] \quad (2)$$

A K value of 36 ± 1 M^{-1} at 25 °C was estimated from the intercept of the log–log plot (Fig. S9†), using data up to the solubility limit of H_2O in CH_2Cl_2 (~0.13 M)[32] at this temperature, the value being based on repeat experiments (Appendix B); the 1.06 slope of the plot is consistent with a 1 : 1 equilibrium. A more approximate K value of ~10 M^{-1} was estimated from the ^1H NMR spectra of **2a** in CD_2Cl_2 at 25 °C. UV-Vis analysis in C_6H_6 gave a K value of ~28 M^{-1} (Appendix B), reasonable agreement with the 36 M^{-1} value, implying perhaps that CH_2Cl_2 and C_6H_6 are likely both non-coordinating toward **1a** (or have similar, weak binding properties). K values in CH_2Cl_2 were measured from 10 to 38 °C, but reproducible values at the extreme temperatures could not be obtained. Nevertheless, ΔH^o, ΔS^o and ΔG^o values were estimated to be, respectively, −50 ± 20 kJ mol^{-1}, −140 ± 40 kJ mol^{-1}, and −8.9 ± 0.2 kJ mol^{-1} (at 25 °C, based on K = 36 ± 1 M^{-1}) for the coordination of H_2O to **1a** (see Appendix B); the exothermicity and negative entropy are consistent with an equilibrium such as eqn (1).[1] Comparison of the K = 36 M^{-1} value with corresponding values obtained for the S-ligand systems (in C_6D_6)[1] indicates that the formation of $RuCl_2$(P–N)(PPh_3)L is favoured in the order: L = MeSH > EtSH ~ H_2S > H_2O, with K decreasing from 296 to 36 M^{-1}. Kinetic studies on ligand substitution were attempted, for example, by exposing solutions of **2a** (in acetone containing >1.0 M H_2O, or in CH_2Cl_2 solution containing 0.13 M H_2O) to 1 atm H_2S. However, the solution changed 'instantaneously' from pink to the yellow colour of the H_2S adduct,[1] and the reaction rates were too rapid to be measured.

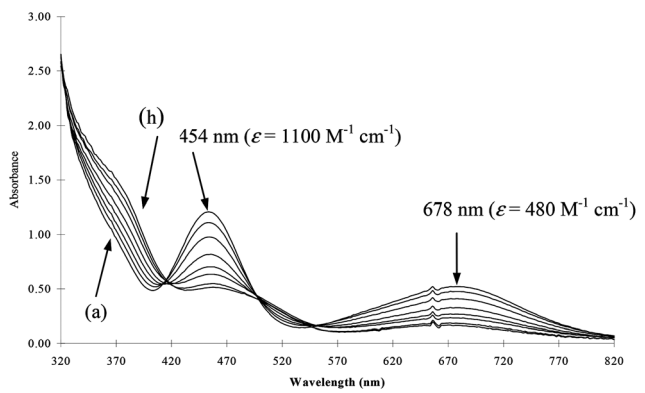

Fig. 4 Spectral changes observed upon addition of H_2O to $RuCl_2$(P–N)(PPh_3) (**1a**) (1.04 × 10^{-3} M) in CH_2Cl_2 at 25 °C. Added [H_2O] = (a) 0.0, (b) 0.0056, (c) 0.0111, (d) 0.0333, (e) 0.0500, (f) 0.0666, (g) 0.0999, (h) 0.1110 M.

The alcohol complexes

Syntheses of the *trans*-$RuCl_2$(P–N)(PPh_3)(ROH) adducts (**3**, R = Me; and **4**, R = Et) were complicated as trace moisture led to formation of the aqua adduct **2a**, but the pink complex **3** of good elemental analysis was eventually isolated in 56% yield from a mixture of $RuCl_2(PPh_3)_3$ and P–N in a vigorously dried 2 : 5 blend of MeOH and acetone. The $^{31}P\{^1H\}$ NMR spectrum of isolated **3** in CD_2Cl_2 was similar to that of **2a** (*cf.* Fig. S3†), and again implies an equilibrium with **1a** but, in the presence of 50 equiv. of MeOH, both P_A and P_X signals were seen as doublets at δ ~77 and ~47, respectively, with $^2J_{PP}$ = 36.7 Hz. The ^1H NMR data (Fig. S10) are similar to those of **2a**, and are consistent with the *trans* structure. Isolation of analytically pure **4** was not achieved by mixing $RuCl_2(PPh_3)_3$ and P–N over long periods in EtOH-containing, mixed solvents. An uncharacterized, insoluble, brown solid was first readily isolated and, after a lengthy work-up procedure, a pink compound was subsequently isolated in 33% yield from the filtrate. NMR spectra in CD_2Cl_2 of this pink solid (*e.g.* Fig. 5) showed the absence of impurities and are completely consistent with the EtOH adduct, but the C-analysis is 1.0% high, almost certainly due to contamination by hexanes used for washing; attempts to achieve more effective drying were foiled by accompanying loss of the EtOH, noted visibly by colour changes. Rapid reversible coordination of the alcohol in solution is apparent from the $^{31}P\{^1H\}$ NMR spectrum, and the variable temperature NMR data for **4** again resemble those of **2a**.

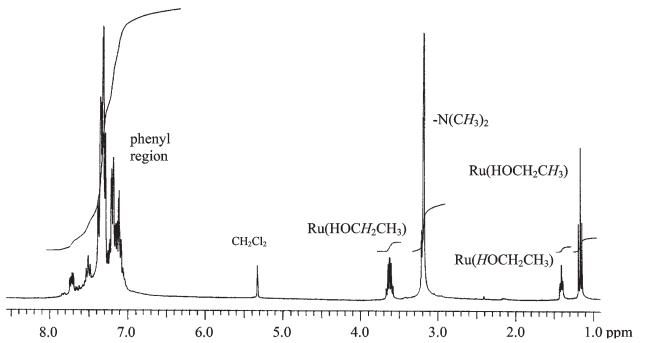

Fig. 5 ^1H NMR spectrum (300 MHz) of *trans*-$RuCl_2$(P–N)(PPh_3)(EtOH) (**4**) in CD_2Cl_2 at r.t.

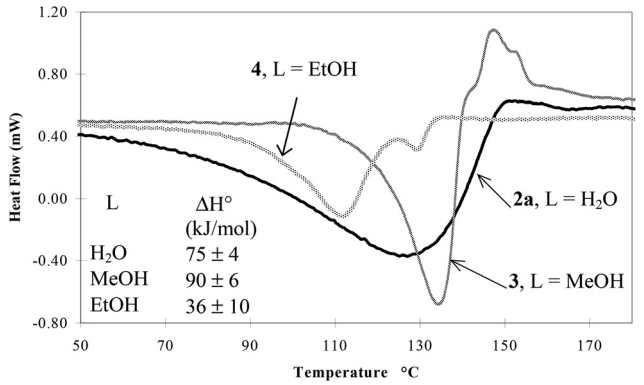

Fig. 6 DSC curves for *trans*-$RuCl_2(P–N)(PPh_3)L$ complexes. Greater error in ΔH^o for 4 results from the inability of obtaining it analytically pure (see text).

The alcohol adducts are isolated only under absolutely anhydrous conditions and, even in the solid state under 1 atm Ar, the complexes lose the solvent to regenerate the green, five-coordinate **1a**.

Stabilization of octahedral Ru^{II}–phosphine complexes by the presence of MeOH and EtOH ligands has been known for decades, for example. as in $RuCl_2(EtOH)(PMe_2Ph)_3$,[33] $[RuH(PPh_3)_2(H_2O)_2(MeOH)]^+$,[34] $[Ru(Y)Cl_2(MeOH)(PPh_3)_2]$ (Y = CO or CS),[35] $[RuH(PMe_2Ph)_4(MeOH)]^+$,[36] and $[RuH(dppe)_2(EtOH)]^+$,[36] and our findings now extend this to a P–N coordinated species. A labile alcohol ligand can play a key role in catalysis, as exemplified within a Ru-BINAP-MeOH species used for homogeneous asymmetric hydrogenation.[37]

Differential scanning calorimetry (DSC) data

The ΔH^o values for dissociation of the H_2O, MeOH and EtOH from the respective complexes *cis*-**2a**, -**3** and -**4** to give **1a** were obtained from DSC experiments (Fig. 6). Taken together with our earlier DSC data for dissociation of the S-ligands from the *trans* complexes,[1] ΔH^o is seen to decrease in the order: MeSH (94 kJ mol^{-1}) > MeOH (90) > H_2S (85) > H_2O (75) > EtSH (64) > EtOH (36). Thus, in the solid state, the S-ligands, which are *trans* to Cl, require higher dissociation energy than the corresponding O-ligands, which are *trans* to P_A, a site of strong *trans*-influence (see above). The MeSH[1] and MeOH adducts are noticeably more thermally stable than the other complexes, perhaps because these Me-containing molecules are of the most compatible size and electronic structure to occupy the vacant site. The ΔH^o value of -75 ± 4 kJ mol^{-1} for coordination of H_2O to **1a** in the solid state compares with the more questionable value of -50 ± 20 kJ mol^{-1} estimated in CH_2Cl_2 solution (see above); if there is any real difference in these values, weak bonding of the CH_2Cl_2 could be a factor, since Ru^{II}–CH_2Cl_2 complexes are known.[38] Finally, DSC data for **2b**, the *p*-tolyl analogue of **2a**, give a value of 62 ± 2 kJ mol^{-1} for removal of the H_2O ligand (Fig. S11†), the number being consistent with the longer Ru–O bond in **2b** (2.252 Å) than in those determined in the structures of the benzene solvates of **2a** (2.229 and 2.189 Å). It should be noted that **1a** also reversibly binds N_2 and N_2O to generate *cis*-species, but the coordination is weaker than with the oxygen- and sulfur-donor ligands.[2a,39]

Conclusions

The ability of square pyramidal complexes of the type *trans*-$RuCl_2(P–N)(PR_3)$, where R is Ph or *p*-tolyl, to bind small molecules is extended to include water, MeOH and EtOH. The study of formation of the *trans*-products, together with previously reported findings for the binding of H_2, N_2, N_2O, H_2S, MeSH and EtSH, which all form *cis*-products, uniquely illustrates formation of six-coordinate products from a five-coordinate precursor with such a range of small molecules. Crystallographic and thermodynamic data (in both solution and the solid state) for the reversible equilibria systems allow for creation of trends describing *trans*-influence and insight into the bond strengths of the small molecule ligands. The five-coordinate precursor also reacts with NH_3, CO and acetylenes but these systems lead to more than a single product, chemistry that will be described elsewhere.

Acknowledgements

We thank the Natural Sciences and Engineering Council of Canada for funding and Colonial Metals Inc. for a loan of $RuCl_3 \cdot xH_2O$.

References

1 E. S. F. Ma, S. J. Rettig, B. O. Patrick and B. R. James, *Inorg. Chem.*, 2012, **51**, 5427.
2 (*a*) D. C. Mudalige, S. J. Rettig, B. R. James and W. R. Cullen, *J. Chem. Soc., Chem. Commun.*, 1993, 830; (*b*) D. C. Mudalige, E. S. F. Ma, S. J. Rettig, B. R. James and W. R. Cullen, *Inorg. Chem.*, 1997, **36**, 5426.
3 (*a*) D. C. Mudalige, PhD thesis, The University of British Columbia, Vancouver, British Columbia, Canada, 1994; (*b*) E. S. F. Ma, PhD thesis, The University of British Columbia, Vancouver, British Columbia, Canada, 1999.
4 D. D. Perrin, W. L. F. Armarego and D. R. Perrin, *Purification of Laboratory Chemicals*, Pergamon, Oxford, 2nd edn, 1980.
5 P. S. Hallman, T. A. Stephenson and G. Wilkinson, *Inorg. Synth.*, 1970, **12**, 237.
6 P. W. Armit, W. J. Sime, T. A. Stephenson and L. Scott, *J. Organomet. Chem.*, 1978, **161**, 391.
7 *d*TREK. Area Detector Software, version 4.13*, Molecular Structure Corp, The Woodlands, TX, 1996–1998.
8 A. Altomare, M. C. Burla, M. Camalli, G. L. Cascarano, C. Giacovazzo, A. Guagliardi, A. G. G. Moliterni, G. Polidori and R. Spagna, *J. Appl. Crystallogr.*, 1999, **32**, 115.
9 G. M. Sheldrick, *Acta Crystallogr., Sect. A: Found. Crystallogr.*, 2008, **64**, 112.

10 *WinGX-V1.80.05*; L. J. Farrugia, *J. Appl. Crystallogr.*, 1999, **32**, 837.
11 C. Schotes, M. Ranocchiari and A. Mezzetti, *Organometallics*, 2011, **30**, 3596.
12 (*a*) H. J. Lawson, T. S. Janik, M. R. Churchill and K. J. Takeuchi, *Inorg. Chim. Acta*, 1990, **174**, 197; (*b*) S. K. Mandal and A. R. Chakravarty, *Inorg. Chem.*, 1993, **32**, 3851.
13 S. M. Boniface, G. R. Clark, T. J. Collins and W. R. Roper, *J. Organomet. Chem.*, 1981, **206**, 109.
14 M. S. Röthlisberger, W. Hummel, P.-A. Pittet, H.-B. Bürgi, A. Ludi and A. E. Merbach, *Inorg. Chem.*, 1988, **27**, 1358.
15 D. V. McGrath and R. H. Grubbs, *J. Am. Chem. Soc.*, 1991, **113**, 3611.
16 P. Bernhard, H.-B. Bürgi, J. Hauser, H. Lehmann and A. Ludi, *Inorg. Chem.*, 1982, **21**, 3936.
17 U. Kölle, G. Flunkert, R. Görissen, M. U. Schmidt and U. Englert, *Angew. Chem., Int. Ed. Engl.*, 1992, **31**, 440.
18 H. Basch, M. Krauss, W. J. Stevens and D. Cohen, *Inorg. Chem.*, 1985, **24**, 3313.
19 S. Shinoda, Y. Koie and Y. Saito, *Bull. Chem. Soc. Jpn.*, 1986, **59**, 2938.
20 E. S. Ma, S. J. Rettig and B. R. James, *Chem. Commun.*, 1999, 2463.
21 A. J. Deeming and G. P. Proud, *Inorg. Chim. Acta*, 1985, **100**, 223.
22 A. J. Deeming, G. P. Proud, H. M. Dawes and M. B. Hursthouse, *J. Chem. Soc., Dalton Trans.*, 1986, 2545.
23 (*a*) J. Malito and E. C. Alyea, *Transition Met. Chem.*, 1992, **17**, 481; (*b*) G. K. Anderson and R. Kumar, *J. Chem. Res. (S)*, 1998, 48.G. K. Anderson and R. Kumar, *J. Chem. Res. (M)*, 1988, 432.
24 (*a*) E. Grimley and D. W. Meek, *Inorg. Chem.*, 1986, **25**, 2049; (*b*) P. Brüggeller, *Inorg. Chem.*, 1987, **26**, 4125.
25 (*a*) A. Pidcock, R. E. Richards and L. M. Venanzi, *J. Chem. Soc. A*, 1966, 1707; (*b*) J. J. Gambaro, W. H. Hohman and D. W. Meek, *Inorg. Chem.*, 1989, **28**, 4154.
26 K. D. Tau and D. W. Meek, *Inorg. Chem.*, 1979, **18**, 3574.
27 R. L. Keiter and J. G. Verkade, *Inorg. Chem.*, 1969, **8**, 2115.
28 P. G. Jessop, S. J. Rettig, C.-L. Lee and B. R. James, *Inorg. Chem.*, 1991, **30**, 4617.
29 (*a*) K. S. MacFarlane, A. M. Joshi, S. J. Rettig and B. R. James, *Inorg. Chem.*, 1996, **35**, 7304; (*b*) S. L. Queiroz, A. A. Batista, G. Oliva, M. T. Do, P. Gambardella, R. H. A. Santos, K. S. MacFarlane, S. J. Rettig and B. R. James, *Inorg. Chim. Acta*, 1998, **267**, 209.
30 A. J. Deeming, S. Doherty, J. E. Marshall, J. L. Powell and A. M. Senior, *J. Chem. Soc., Dalton Trans.*, 1993, 1093.
31 The isosbestic points in Fig. 4 are not quite as sharp as those usually seen on the HP 8452 instrument, but the excellent log : log plot (Fig. S9†) from the Fig. 4 data has the correct slope, and the *K* value is well determined. The isosbestics seen in Fig. S6–S8† for spectra in C_6H_6, acetone, and THF, respectively, are sharper.
32 *IUPAC Solubility Data Series, Vol. 60, Halogenated Methanes with Water*, ed. A. L. Horváth and F. W. Getzen, Oxford University Press, Oxford, 1995, p. 153.
33 J. Chatt, G. J. Leigh and R. J. Paske, *J. Chem. Soc. A*, 1969, 854.
34 R. J. Young and G. Wilkinson, *J. Chem. Soc., Dalton Trans.*, 1976, 719.
35 P. W. Armit, W. J. Sime and T. A. Stephenson, *J. Chem. Soc., Dalton Trans.*, 1976, 2121.
36 T. V. Ashworth and E. Singleton, *J. Chem. Soc., Chem. Commun.*, 1976, 706.
37 C.-C. Chen, T.-T. Huang, C.-W. Lin, R. Cao, A. S. C. Chan and W. T. Wong, *Inorg. Chim. Acta*, 1998, **270**, 247.
38 (*a*) D. Huang, J. C. Huffman, J. C. Bollinger, O. Eisenstein and K. G. Caulton, *J. Am. Chem. Soc.*, 1997, **119**, 7398; (*b*) J. Zhang, K. A. Barakat, T. R. Cundari, T. B. Gunnoe, P. D. Boyle, J. L. Petersen and C. S. Day, *Inorg. Chem.*, 2005, **44**, 8379.
39 C. B. Pamplin, E. S. F. Ma, N. Safari, S. J. Rettig and B. R. James, *J. Am. Chem. Soc.*, 2001, **123**, 8596.

